Optical shock wave and photon-number conservation

A. M. Zheltikov

Department of Physics and Astronomy, Texas A&M University, College Station, Texas 77843, USA;
Physics Department, International Laser Center, M. V. Lomonosov Moscow State University, Moscow 119992, Russia;
Russian Quantum Center, ul. Novaya 100, Skolkovo, Moscow Region, 143025 Russia;
and Kazan Quantum Center, A.N. Tupolev Kazan National Research Technological University, Kazan 420126, Russia

The nonlinear Schrödinger equation (NSE) provides a powerful tool for the analysis of ultrafast nonlinear-optical dynamics, including a vast class of optical solitons. Here, we show, however, that the photon-number integral of the NSE differs from the physical number of photons, conserved by more general field evolution equations. This difficulty is traced to the optical shock term, which is dropped in the NSE, making nonlinear coupling in NSE-based models frequency independent and leading to unphysical predictions for ultrabroadband, octave-spanning field waveforms.

I. INTRODUCTION

The photon number is one of the key parameters in the quantum treatment of optical fields. In quantum optics, photon-number analysis is central to the understanding and characterization of a vast class of quantum states of light [1,2]. In nonlinear optics, such analysis helps identify fundamental conservation laws [3,4], providing important physical insights into the limitations on frequency conversion efficiency in optical parametric amplification, as well as in sum- and difference-frequency generation processes [5].

Although the number operator is consistently defined for a broad class of quantizable fields [6], the photon number in its most physically transparent form is defined as a product of operators creating and annihilating photons of well-defined frequency [1,2]. This definition of the photon number is broadly accepted for the analysis of a vast variety of quantum-optic phenomena, including squeezed light and quantum entanglement, as well as quantum information processing, storage, and communication schemes [7–9].

Ultrafast optical physics, however, operates with broadband photon packets [10,11]. Nonlinear-optical interactions of ultrashort laser pulses often involve multiple energy-exchange pathways coupling photon packets that belong to fundamentally inseparable spectral-temporal modes of the optical field [12,13]. Spectral and temporal transformation of optical field waveforms with octave- and multioctave-spanning spectra, referred to as supercontinuum radiation [14–17], is one of the most prominent examples of nonlinear dynamics of this type. With energy exchange occurring in unresolved spectral-temporal modes of the classical field, standard photon-number conservation laws become inapplicable. This leaves a disconcerting no man's land in the realm of quantum nonlinear optics where the concepts and machinery of quantum physics would be needed most to help extend concepts and methods of ultrafast lightwave technologies to the rapidly growing and highly promising area of single-photon nonlinear optics [18–21].

Here, we focus on photon-number conservation in the nonlinear wave dynamics of broadband optical field wave-forms and their quantum-field counterparts—broadband photon packets. Within a vast parameter space, the classical-field evolution of such waveforms is described by the nonlinear Schrödinger equation (NSE). The quantized version of the NSE provides a powerful tool for the description of a broad variety of quantum nonlinear-optical processes. A vast class of physically significant and practically important phenomena in ultrafast nonlinear optics, including a broad variety of soliton regimes and elementary self-phase modulation (SPM) scenarios, is adequately described in terms of NSE field waveform solutions with symmetrically broadened spectra and symmetric pulse shapes. Here, we show, however, that the spectral and temporal symmetry of NSE solutions is inconsistent with simultaneous energy and photon-number conservation. We will also demonstrate that the photon-number integral of the NSE differs from the physical number of photons, conserved by more general field evolution equations. This difficulty is traced to the optical shock term, which is dropped in the NSE, making nonlinear coupling in NSE-based models frequency independent and leading to unphysical predictions in the case of ultrabroadband, octave-spanning field waveforms.

II. FIELD EVOLUTION EQUATIONS

For the sake of definiteness, we focus here on the nonlinear dynamics of broadband field waveforms in optical fibers. With the guided-wave geometry in mind, we represent the Fourier transform of the field as [3,22]

$$E(\omega, x, y, z) = F(\omega, x, y)A(\omega, z), \qquad (1)$$

where x and y are the transverse coordinates, z is the longitudinal coordinate, ω is the frequency, and $F(\omega, x, y)$ is the dimensionless function describing the transverse field profile found by solving the transverse part of the wave equation.

A generic frequency-domain equation for the unidirectional evolution of an ultrashort optical pulse in a medium with a third-order optical nonlinearity is then written

as [22,23]

$$i\frac{\partial}{\partial z}A(\omega, z) = [\beta(\omega) - \beta(\omega_0)]A(\omega, z) + \Gamma P(\omega). \quad (2)$$

Here, $\beta(\omega)$ is the propagation constant, ω_0 is the central frequency of the input laser field, $\Gamma = 2\pi\sigma\chi^{(3)}\omega^2/[c^2\beta(\omega)]$, $P(\omega) = \hat{F}\{A(t, z)\int f(t - \theta)|A(\theta, z)|^2 d\theta\}$, $A(\theta, z)$ is the time-domain field amplitude found as a Fourier transform of $A(\omega, z)$, $\chi^{(3)}$ is the pertinent third-order susceptibility, $\hat{F}\{\bullet\}$ is the Fourier-transform operator, c is the speed of light in vacuum, $\sigma = \int[F(x, y)]^4 dxdy/\int[F(x, y)]^2 dxdy$, $f(\theta) = \varepsilon\delta(\theta) + (1 - \varepsilon)R(\theta)$, $R(\theta)$ is the Raman response function, and ε and $1 - \varepsilon$ are the fractions of the instantaneous (Kerr) and delayed (Raman) nonlinearity in the overall nonlinear response. The Raman effect involves inelastic scattering of light, which does not conserve energy, as some energy of the optical field is spent on the excitation of a Raman-active vibration.

When transformed to the time domain, Eq. (2) leads to the generalized nonlinear Schrödinger equation (GNSE) [22,23]

$$i\frac{\partial}{\partial z}A(\eta, z) + \sum_{k \geq 2}\frac{(i)^k}{k!}\beta_k\frac{\partial^k}{\partial \eta^k}A(\eta, z)$$

$$= \kappa_0\sigma(1 - \hat{S})A(\eta, z)\int f(\eta - \theta)|A(\theta, z)|^2 d\theta, \quad (3)$$

where η is the time in the retarded frame of reference, $\kappa_0 = n_2\omega_0/c$, $n_2 = 2\pi\chi^{(3)}/n_{\text{eff}}$, $n_{\text{eff}} = c\beta/\omega$, $\beta_k = \partial^k\beta/\partial\omega^k|_{\omega_0}$, and

$$\hat{S} = \frac{i}{\omega_0}\frac{\partial}{\partial\eta} + i\frac{\partial}{\partial\omega}\ln\left(\frac{\sigma}{n_{\text{eff}}}\right)\frac{\partial}{\partial\eta}. \quad (4)$$

To reduce the full field evolution equation (3) to the NSE [22],

$$i\frac{\partial}{\partial z}A(\eta, z) - \frac{\beta_2}{2}\frac{\partial^2}{\partial\eta^2}A(\eta, z) = \kappa_0\sigma A(\eta, z)|A(\eta, z)|^2, \quad (5)$$

one needs to truncate the sum in k on the left-hand side of Eq. (3) to the $k = 2$ term, require the nonlinearity to be purely instantaneous, $\varepsilon = 1$, and set $\hat{S} = 0$. The truncation of the sum in k in Eq. (3) is equivalent to neglecting high-order dispersion effects. The $\varepsilon = 1$ condition implies that the Raman effect is ignored and the entire nonlinear response is assumed to be instantaneous, which is not always justified [24]. Finally, setting $\hat{S} = 0$, we ignore the frequency dependence of the nonlinear coupling constant and neglect shock-wave effects.

Spectrally symmetric broadening is an important feature that is common of a broad class of well-known solutions of Eq. (5), including a family of celebrated soliton solutions [22,25,26]. Specifically, for the fundamental soliton solution, a hyperbolic secant pulse shape translates into a symmetric spectrum of the same hyperbolic secant shape [22,27]. In soliton breathing scenarios [22,25,26], optical waveforms display signature cycles in both the time and frequency domain. As a part of this oscillatory dynamics, the stage of pulse compression and spectral broadening is followed by pulse stretching and spectral compression, in which the pulse exhibits its multisoliton structure.

III. PHOTON-NUMBER CONSERVATION

When the dispersion term is dropped in Eq. (5), the NSE is reduced to a canonical SPM equation. This equation dictates a signature symmetric spectral broadening of a laser pulse [3,4,22], the bandwidth of which undergoes an unbounded growth as a function of the laser peak power, optical nonlinearity, and the propagation distance with no limits from above or below. Quite disconcerting, there is nothing in this theory that would prevent the low-frequency wing of the spectrum from reaching the zero frequency—a big electrodynamic no-no. Notably, when applied to single-cycle field waveforms, the NSE (5) also predicts symmetric spectra that extend all the way down—and even beyond—the zero frequency.

Spectral blueshifting related to pulse self-steepening has long been identified as a key effect that prevents this long-wavelength catastrophe in SPM-induced spectral broadening. Helpful approximate analytical expressions have been derived for the bandwidths of SPM-broadened spectra [28], offering important physical insights into SPM regimes that yield octave-spanning spectra and showing that the zero frequency is happily avoided.

Here, we focus on the fundamental, conservation-law aspects behind this blueshifting effect whereby low frequencies in nonlinearity-broadened octave-spanning spectra are suppressed and the zero frequency is avoided. To this end, we examine the classical photon-number constant of motion of the field evolution equation (2), as identified by Blow and Wood [23]:

$$\frac{\partial}{\partial z}\left[\int\frac{n_{\text{eff}}}{\sigma}\frac{|A(\omega_0 + \Omega, z)|^2}{\omega_0 + \Omega}d\Omega\right] = 0. \quad (6)$$

To relate Eq. (6) to photon-number conservation, we follow a standard field-quantization procedure, treating the spectral field amplitude $A(\omega, z)$ in a waveguide mode with an effective refractive index n_{eff} as an operator [7,9]:

$$\hat{A}(\omega, z) = \left(\frac{\hbar\omega}{n_{\text{eff}}c}\right)^{1/2}\hat{a}(\omega, z), \quad (7)$$

where $\hat{a}(\omega, z)$ is the annihilation operator such that

$$[\hat{a}(\omega, z), \hat{a}^\dagger(\omega', z)] = \delta(\omega - \omega'). \quad (8)$$

The time-domain annihilation operator is defined through a Fourier transform:

$$\hat{a}(t, z) = \frac{1}{(2\pi)^{1/2}}\int\hat{a}(\omega, z)\exp(-i\omega t)d\omega. \quad (9)$$

We also introduce the time- and frequency-domain photon density operators:

$$\hat{n}(\omega, z) = \hat{a}^\dagger(\omega, z)\hat{a}(\omega, z) \quad (10)$$

and

$$\hat{n}(t, z) = \hat{a}^\dagger(t, z)\hat{a}(t, z). \quad (11)$$

Photon density operators defined by Eqs. (10) and (11) have the units of time and frequency, respectively. We can now

combine Eqs. (6), (7), and (10) to find

$$\frac{\partial}{\partial z}\left[\int \frac{\hat{n}(\omega_0 + \Omega, z)}{\sigma}d\Omega\right] = 0. \tag{12}$$

We have kept the $1/\sigma$ factor in Eq. (12) for the sake of accuracy. However, in most cases, this factor can be safely dropped from the constant of motion of Eqs. (6) and (12), as σ is usually a very weak function of the frequency. For a generic Gaussian waveguide mode, σ is plain constant.

Provided that the frequency dependence of σ is negligible, Eq. (12) reduces to

$$\frac{\partial \hat{N}}{\partial z} = \frac{\partial}{\partial z}\left[\int \hat{n}(\omega_0 + \Omega, z)d\Omega\right] = 0. \tag{13}$$

We can see now that, while the single-frequency photon density operator $\hat{n}(\omega, z)$ is not a constant of motion of Eq. (2), the integral of this operator over the entire spectrum is.

It is instructive to compare this result with photon-number conservation in NSE-based models. The NSE Hamiltonian $\hat{H}_0$ is known to commute with the photon-number operator $\hat{N}_0$ [29]. As a consequence, $\hat{N}_0$ is a constant of motion of the input-output Heisenberg evolution equation:

$$\frac{d\hat{N}_0}{dz} = \frac{i}{\hbar}[\hat{H}_0, \hat{N}_0]. \tag{14}$$

We are going to show now that the photon-number operator $\hat{N}_0$ that the NSE Hamiltonian $\hat{H}_0$ commutes with is different from the photon-number operator $\hat{N}$ conserved by the full field evolution equation (2). Unlike Eq. (2), the NSE [Eq. (5)] sets $\hat{S} = 0$. In the spectral representation, this implies that the frequency variable ω in the expression for Γ in the field evolution equation is replaced by the central frequency of the laser pulse ω_0. With such a replacement, the factor $\Gamma = 2\pi\sigma\chi^{(3)}\omega/(cn_{\text{eff}})$ in Eq. (2) becomes $\Gamma_0 = 2\pi\sigma\chi^{(3)}\omega_0/(cn_{\text{eff}})$. We multiply Eq. (2) with Γ replaced with Γ_0 by $\beta(\omega)A^*(\omega, z)/(\sigma\omega_0^2)$, subtract this product from its complex conjugate, and integrate the resulting equation over the entire bandwidth of the laser pulse to find

$$\frac{1}{\omega_0}\frac{\partial}{\partial z}\left[\int \frac{n_{\text{eff}}}{\sigma}|A(\omega_0 + \Omega, z)|^2 d\Omega\right] = 0. \tag{15}$$

When σ can be considered frequency independent, Eq. (15) becomes

$$\frac{1}{\omega_0}\frac{\partial}{\partial z}\left[\int n_{\text{eff}}|A(\omega_0 + \Omega, z)|^2 d\Omega\right] = 0. \tag{16}$$

In quantum terms, Eq. (16) translates into

$$\frac{\partial \hat{N}_0}{\partial z} = \frac{\partial}{\partial z}\int \hat{n}_0(\omega_0 + \Omega, z)d\Omega = 0, \tag{17}$$

where

$$\hat{n}_0(\omega, z) = \hat{a}_0^\dagger(\omega, z)\hat{a}_0(\omega, z) \tag{18}$$

is the photon density and the field is quantized such that

$$\hat{A}(t, z) = \left(\frac{2\pi\hbar\omega_0}{n_{\text{eff}}c}\right)^{1/2}\int \hat{a}_0(\omega, z)\exp\left(-i\omega t\right)d\omega. \tag{19}$$

Unlike the field-quantization procedure defined by Eqs. (7)–(9), field quantization (19) isolates the central frequency ω_0 as a constant preintegral factor. With such a quantization, the pulse-energy operator is expressed as

$$\hat{E}_0(z) = \hbar\omega_0\int \hat{n}(\omega, z)d\omega = \hbar\omega_0\int \hat{n}(t, z)dt = \hbar\omega_0\hat{N}_0(z). \tag{20}$$

We see that, nominally, the NSE conserves both energy and the number of photons. However, the photon number $\hat{N}_0$ conserved by the NSE is different from the photon number $\hat{N}$ corresponding, in the classical domain, to the physical number of photons

$$N(z) = \int n_{\text{eff}}\frac{|A(\omega_0 + \Omega, z)|^2}{\omega_0 + \Omega}d\Omega, \tag{21}$$

conserved by the full field evolution equation (2). Instead, as can be seen from Eq. (20), the NSE conserves the ratio of the pulse-energy integral of motion over $\hbar\omega_0$, with the photon-number conservation equation in NSE-based models, $\partial \hat{N}_0/\partial z = 0$, being a trivial consequence of energy conservation, $\partial \hat{E}_0/\partial z = 0$. In other words, photon-number conservation in NSE-based models operates on an assumption that all the photons have the same frequency ω_0.

IV. MANLEY-ROWE RELATIONS

In this section, we will discuss photon-number conservation in NSE- and GNSE-based models from the viewpoint of Manley-Rowe relations [30,31] and show that, while the photon-number conservation equation (13) is consistent with these relations, its simplified NSE counterpart, expressed by Eq. (17), is not. As a simple yet physically instructive argument, we consider a four-wave mixing (FWM) $\omega_1 + \omega_2 \to \omega_3 + \omega_4$ of spectrally nonoverlapping optical fields with bandwidths Δ_q, such that $\Delta_q < |\omega_q - \omega_p|$, p, $q = 1$, 2, 3, 4. When applied to such a process, Eq. (6) yields

$$\frac{\partial}{\partial z}\sum_{q=1}^4\left[\int_{\omega_q - \Delta_q/2}^{\omega_q + \Delta_q/2} n_{\text{eff}}\frac{|A(\Omega, z)|^2}{\Omega}d\Omega\right] = 0. \tag{22}$$

When the fields are narrowband enough so that $1/\Omega$ and n_{eff} vary slowly within each bandwidth Δ_q compared to the spectral intensity $|A(\Omega, z)|^2$, Eq. (21) gives

$$\frac{\partial}{\partial z}\sum_{q=1}^4\frac{P_q(z)}{\bar{\omega}_q} = 0, \tag{23}$$

where $\bar{\omega}_q \approx \omega_q$ is a median frequency within the bandwidth Δ_q and $P_q(z) = \int_{\omega_q - \Delta_q/2}^{\omega_q + \Delta_q/2}|A(\Omega, z)|^2 d\Omega$.

With Eq. (23) rewritten as

$$\sum_{q=1}^4\frac{\delta P_q(z)}{\bar{\omega}_q} = 0, \tag{24}$$

where $\delta P_q(z) = P_q(z) - P_q(0)$, we arrive at a Manley-Rowe-type relation for the power flows δP_q in individual FWM-coupled fields, valid for any z. When all the four fields are monochromatic, $\bar{\omega}_q = \omega_q$, Eq. (24) becomes a standard Manley-Rowe relation.

Although written for a special case of spectrally isolated narrowband fields, Eq. (24) offers an important insight into Eq. (6) for a classical field and Eq. (13) for a quantized field as Manley-Rowe-type relations. As one of the key results of this analysis, Eq. (6) generalizes the Manley-Rowe relations, formulated in their canonical form for monochromatic fields, to intrapulse nonlinear-optical processes in which an optical nonlinearity couples spectrally unresolved, often overlapping components of an ultrashort laser pulse.

We have also seen that, unlike the full field evolution equation, its simplified NSE counterpart [Eq. (5)] fails to fulfill the Manley-Rowe-type relations of the form of Eq. (6). Connection to the Manley-Rowe relations is lost in NSE-based models at the point where the frequency-dependent coupling factor—Γ in Eq. (2)—is replaced by a frequency-independent constant. In the time domain, this replacement translates into an $\hat{S} = 0$ simplification. With the $\hat{S}$ term dropped and high-order dispersion [terms with $k \geqslant 3$ in Eq. (3)] neglected, NSE-type field evolution equations yield spectrally and temporally symmetric solutions. The spectral symmetry implies that sidebands $\omega_0 \pm \Omega$ have equal spectral intensity, $S(\omega_0 + \Omega) = S(\omega_0 - \Omega)$. On the other hand, with the FWM $\omega_0 + \omega_0 \rightarrow (\omega_0 + \Omega) + (\omega_0 - \Omega)$ being the process behind $\omega_0 \pm \Omega$ sideband generation, the number of $\omega_0 + \Omega$ photons has to be equal to the number of $\omega_0 - \Omega$ photons, $N(\omega_0 + \Omega) = N(\omega_0 - \Omega)$. Since $S(\omega) = \hbar \omega N(\omega)$, the spectral symmetry, $S(\omega_0 + \Omega) = S(\omega_0 - \Omega)$, is incompatible with $N(\omega_0 + \Omega) = N(\omega_0 - \Omega)$ unless $\Omega = 0$. Remarkably, it is precisely the $\Omega = 0$ approximation that enables the NSE-based models. Indeed, the coefficient in front of the nonlinear term in the full pulse evolution equation (2) reads $\kappa = n_2 \omega / c = n_2 (\omega_0 + \Omega)/c$. The NSE of Eq. (5), on the other hand, operates with the nonlinear coupling coefficient $\kappa_0 = n_2 \omega_0 / c$, which is treated as a frequency-independent constant with $\Omega = 0$. Thus, although the NSE is certainly applicable to ultrashort pulses and, moreover, provides a powerful tool for the description of soliton dynamics, it reconciles $S(\omega_0 + \Omega) = S(\omega_0 - \Omega)$ with $N(\omega_0 + \Omega) = N(\omega_0 - \Omega)$ by assigning the same frequency ω_0 to all the frequency components that constitute the spectrum of the pulse. In quantum terms, this allows the pulse energy to be calculated, as suggested by Eq. (20), simply as the number of photons times the photon energy at the central frequency $\hbar \omega_0$.

V. SPECTRAL SYMMETRY AND PHOTON-NUMBER CONSERVATION

Analysis of the Manley-Rowe relations presented in the previous section offers important insights into why NSE-based models fail to simultaneously satisfy energy and photon-number conservation. This analysis is especially instructive when spectral broadening can be traced back to elementary FWM processes, where Stokes and anti-Stokes photons at frequencies $\omega_0 \pm \Omega$ are generated in pairs as a result of annihilation of two pump-field photons at frequency ω_0. However, supercontinuum generation scenarios in optical fibers and laser filaments are often much more complicated.

In this section, we focus on the spectral and temporal symmetry of NSE solutions and show that this symmetry is inconsistent with simultaneous energy and photon-number

conservation. To this end, we represent the energy and the photon number as

$$E(z) = \int_0^\infty S(\omega_0 + \Omega, z)d\Omega + \int_0^\infty S(\omega_0 - \Omega, z)d\Omega, \tag{25}$$

$$N(z) = \int_0^\infty \frac{S(\omega_0 + \Omega, z)}{\hbar(\omega_0 + \Omega)}d\Omega + \int_0^\infty \frac{S(\omega_0 - \Omega, z)}{\hbar(\omega_0 - \Omega)}d\Omega, \tag{26}$$

where $S(\omega, z)$ is the spectral density, which changes as a function of z due to optical nonlinearity as prescribed by the appropriate field evolution equation.

The energy and photon-number conservation equations can then be written as

$$E(z) = \int_0^\infty S(\omega_0 + \Omega, 0)d\Omega + \int_0^\infty S(\omega_0 - \Omega, 0)d\Omega = E_0, \tag{27}$$

$$N(z) = \int_0^\infty \frac{S(\omega_0 + \Omega, 0)}{\hbar(\omega_0 + \Omega)}d\Omega + \int_0^\infty \frac{S(\omega_0 - \Omega, 0)}{\hbar(\omega_0 - \Omega)}d\Omega = N_0. \tag{28}$$

If the field evolution equation yields a solution with symmetric spectrum, so that for any z $S(\omega_0 + \Omega, z) = S(\omega_0 - \Omega, z)$, the energy conservation equation (27) gives

$$E(z) = 2\int_0^\infty S(\omega_0 + \Omega, z)d\Omega$$
$$= 2\int_0^\infty S(\omega_0 + \Omega, 0)d\Omega = E_0. \tag{29}$$

The number of photons as a function of z is then given by

$$N(z) = \frac{2}{\hbar \omega_0} \int_0^\infty \frac{S(\omega_0 + \Omega, z)}{1 - \frac{\Omega^2}{\omega_0^2}}d\Omega. \tag{30}$$

We first consider the FWM process $\omega_0 + \omega_0 \rightarrow (\omega_0 + \Omega_0) + (\omega_0 - \Omega_0)$, in which two pump-field photons at frequency ω_0 are converted to Stokes and anti-Stokes photons at frequencies $\omega_0 \pm \Omega_0$. To model this process, we take $S(\omega_0 + \Omega, 0) = s_0 \delta(\omega_0)$ and $S_\pm(\omega_0 \pm \Omega_0, z) = s_\pm \delta(\omega_0 \pm \Omega_0)$.

When applied to a pulse with such a spectrum and combined with the requirement of spectral symmetry, $S(\omega_0 + \Omega, z) = S(\omega_0 - \Omega, z)$, the energy conservation equation (29) gives $s_+ = s_- = s_0 = E_0/2$. Equation (30) for the number of photons, on the other hand, leads to $N_0 = N(0) = 2s_0/(\hbar \omega_0) = E_0/(\hbar \omega_0)$. Taking the integral in Eq. (30), we find

$$N(z) = \frac{E_0}{\hbar \omega_0} \frac{1}{1 - \frac{\Omega_0^2}{\omega_0^2}} = \frac{N_0}{1 - \frac{\Omega_0^2}{\omega_0^2}}. \tag{31}$$

As can be seen from Eq. (31), $N(z) > N_0$ for any nonzero Ω_0, showing that the condition of photon-number conservation [Eq. (28)] is not satisfied.

Next, we consider a laser pulse with a flat spectrum the bandwidth $\Delta(z)$ of which is a growing function of z, reflecting

the spectral broadening of the pulse. When applied to a pulse with such a spectrum, the energy conservation equation (27) gives $2\int_0^{\Delta(z)} S(\omega_0 + \Omega, z)d\Omega = 2S(z)\Delta(z) = E_0$. Equation (30) for the number of photons then leads to

$$N(z) = \frac{E_0}{\hbar\omega_0}\frac{\omega_0^2}{\Delta(z)}\int_0^{\Delta(z)}\frac{d\Omega}{\omega_0^2 - \Omega^2}. \qquad (32)$$

Taking the integral in Eq. (32), we find

$$N(z) = \frac{E_0}{\hbar\omega_0}\frac{\omega_0}{\Delta(z)}\ln\left|\frac{\Delta(z) + \omega_0}{\Delta(z) - \omega_0}\right|^{1/2}. \qquad (33)$$

In the limiting case of $\Delta(z) \ll \omega_0$, $\zeta(z) = \ln|[\Delta(z) + \omega_0]/[\Delta(z) - \omega_0]|^{1/2} \approx \Delta(z)/\omega_0$, and Eq. (33) reduces to $N(z) \approx E_0/(\hbar\omega_0) \approx N_0$. Thus, in this approximation, the photon number is an integral of motion. However, in a more general case, when the spectral broadening can no longer be included by keeping only the first term in the Taylor-series expansion of the natural logarithm in Eq. (33), the photon number, as can be seen from this equation, becomes a function of the propagation path z and is no longer a constant of motion. In a particular case of broader but still small bandwidths, such that $\zeta(z) \approx \Delta(z)/\omega_0 + (1/3)[\Delta(z)/\omega_0]^3$, Eq. (33) yields

$$N(z) \approx \frac{E_0}{\hbar\omega_0}\left\{1 + \frac{1}{3}\left[\frac{\Delta(z)}{\omega_0}\right]^2\right\}. \qquad (34)$$

In this regime, the photon number does not remain constant, but grows quadratically with $\Delta(z)/\omega_0$.

We consider now a more general case when the pulse bandwidth is small enough so that the Taylor-series expansion $(1 - \Omega^2/\omega_0^2)^{-1} \approx 1 + \Omega^2/\omega_0^2$ can be used in the integrand in Eq. (30). Integration in Eq. (30) then yields

$$N(z) \approx \frac{2}{\hbar\omega_0}\int_0^\infty S(\omega_0 + \Omega, z)\left(1 + \frac{\Omega^2}{\omega_0^2}\right)d\Omega. \qquad (35)$$

With Eq. (29) taken into account,

$$N(z) \approx \frac{E_0}{\hbar\omega_0} + \frac{2}{\hbar\omega_0}\int_0^\infty S(\omega_0 + \Omega, z)\frac{\Omega^2}{\omega_0^2}d\Omega. \qquad (36)$$

In the particular case of a flat spectrum with a bandwidth $\Delta(z)$, Eq. (36) recovers Eq. (34). In its general form, Eq. (36) is, of course, much more general as it is applicable within a much broader class of spectral profiles. As an important result, since the second term in Eq. (36) is positive definite, we find that $N(z) \geqslant E_0/(\hbar\omega_0)$ and the photon number is a growing function of z within the entire range of applicability of Eqs. (35) and (36). This result, obtained here analytically, is confirmed by numerical simulations, presented below in this paper.

VI. OPTICAL SHOCK AND ASYMMETRY OF SPECTRAL-TEMPORAL MODES

To show how frequency-dependent nonlinear wave coupling, translating into the shock term in the time-domain field evolution equation [Eq. (3)], suppresses low-frequency generation as a part of spectral broadening, eventually limiting the spectral bandwidth from below, we use the following

elementary SPM-theory estimate on the nonlinearity-induced spectral broadening [3,22]:

$$\Delta\omega_0 \approx \kappa_0\frac{I}{\tau_0}z, \qquad (37)$$

where I is the field intensity and τ_0 is the pulse width. Equation (37) predicts an unbounded growth of the spectral bandwidth as a function of the propagation length z, field intensity I, and nonlinearity n_2.

We now replace κ_0 in Eq. (37) by the frequency-dependent coupling coefficient $\kappa = n_2\omega/c$ to find for the Stokes and anti-Stokes parts of SPM broadening

$$|\Delta\omega_\pm| \approx \frac{1}{2}\frac{\omega_0 \pm |\Delta\omega_\pm|}{c\tau_0}n_2Iz. \qquad (38)$$

Solving this equation for $|\Delta\omega_\pm|$, we find

$$|\Delta\omega_\pm| \approx \frac{|Q|/2}{1 \mp |Q|/2}\omega_0, \qquad (39)$$

where $Q = n_2Iz/(c\tau_0)$.

An estimate of Eq. (39) is valid only for $|Q| < 1$. For $|Q| \ll 1$, Eq. (39) gives

$$\Delta\omega_\pm \approx \pm\frac{|Q|}{2}\omega_0\left(1 \pm \frac{|Q|}{2}\right). \qquad (40)$$

It is remarkable and encouraging that this elementary qualitative treatment reproduces the key results of a much more rigorous analysis of extreme regime of SPM-induced broadening [28]. Indeed, when applied to a field $A(t, z) = |A(t, z)|\exp[i\varphi(t, z)]$, Eq. (3) with $\beta_k = 0$ for $k \geqslant 2$ and $\varepsilon = 1$ yields the following set of coupled equations for the field amplitude $|A(t, z)|$ and phase $\varphi(t, z)$:

$$\left[\frac{\partial}{\partial z} + \frac{n_{\text{eff}}}{c}\left(1 + \frac{n_2}{n_{\text{eff}}}|A|^2\right)\frac{\partial}{\partial t}\right]|A| = 0 \qquad (41)$$

and

$$\left[\frac{\partial}{\partial z} + \frac{n_{\text{eff}}}{c}\left(1 + \frac{n_2}{n_{\text{eff}}}|A|^2\right)\frac{\partial}{\partial t}\right]\varphi = \frac{n_2\omega_0}{c}|A|^2. \qquad (42)$$

We solve Eqs. (41) and (42) iteratively, neglecting pulse-shape changes in the first-order approximation. With the boundary conditions set as $|A(t, 0)|^2 = A_0^2/\cosh(t/\tau_0)$ and $\varphi(t, 0) = 0$, the solution of Eq. (42) for the phase is then written as [28]

$$\varphi(\eta, z) = \omega_0\eta - \omega_0\tau_0\sinh^{-1}\left[\sinh(\eta/\tau_0) - \frac{n_2}{c\tau_0}A_0^2z\right]. \qquad (43)$$

The resulting spectral broadening is

$$\frac{\Delta\omega(\eta, z)}{\omega_0} = -\frac{1}{\omega_0}\frac{\partial\varphi(\eta, z)}{\partial t} = \frac{1}{\left[1 + \left(\frac{Q^2 - 2Q\sinh(\eta/\tau_0)}{\cosh^2(\eta/\tau_0)}\right)\right]^{1/2}} - 1. \qquad (44)$$

Equation (44) leads to the following expressions for the maximum Stokes and anti-Stokes shifts [28]:

$$\frac{\Delta\omega_\pm}{\omega_0} = \frac{1}{2}[(Q^2 + 4)^{1/2} \pm |Q|] - 1. \qquad (45)$$

For $|Q| \ll 1$, Eq. (45) yields

$$\Delta\omega_{\pm} \approx \pm \frac{|Q|}{2}\omega_0\left(1 \pm \frac{|Q|}{4}\right). \tag{46}$$

It is instructive to compare Eq. (46), which has been derived through the analysis of the first-order solution to Eq. (42) for the phase $\varphi(t, z)$, with Eq. (40), obtained by using much simpler qualitative arguments. Remarkably, Eqs. (40) and (46) differ only by a numerical factor of $1/2$ in front of the small, $\sim |Q|^2$ correction. When only the leading term is kept in Eqs. (40) and (46), both equations recover the standard result of the elementary SPM theory, $\Delta\omega_{\pm} \approx \pm|Q|\omega_0/2$. As $|Q|$ increases, due to a growth in the propagation length, input field intensity, or nonlinearity n_2, the Stokes part of SPM-induced broadening becomes suppressed, while its anti-Stokes counterpart is enhanced, giving rise to an asymmetry in SPM-broadened spectra. In contrast to the elementary SPM theory, which, as can be seen from Eq. (37), does not set any upper bound on $\Delta\omega$ or, hence, on $|\Delta\omega_-|$, Eqs. (40) and (46) prohibit spectral broadening down to the zero frequency. Indeed, reaching this frequency would require $|\Delta\omega_-| = \omega_0$. This condition, however, can never be fulfilled, according to Eqs. (40) and (46), due to the growing $\sim |Q|^2$ correction, which makes sure that spectral broadening is asymmetric so that $|\Delta\omega_-|$ is always smaller than ω_0.

As another important insight, our qualitative treatment of spectral broadening based on Eqs. (38)–(40) provides a reasonably accurate estimate on the propagation length within which spectral broadening ceases to be symmetric. To estimate this spatial scale, we observe that $Q = 1$ is achieved at

$$l_0 \approx c\tau_0/(n_2 I) = 2\pi\,(\tau_0/T_0)l_{\mathrm{NL}}, \tag{47}$$

where T_0 is the field cycle and $l_{\mathrm{NL}} = c/(\omega_0 n_2 I)$ is the nonlinear length.

Equation (47) exactly recovers the spatial scale [22] within which a shock wave tends to build up at one of the pulse edges (the trailing edge of the pulse for $n_2 > 0$), leading to pulse self-steepening. Importantly, neither our qualitative treatment [with Eqs. (38)–(40)] nor the first-order solution of the coupled equations (41) and (42) implies or assumes any pulse distortion. On the contrary, when searching for the first-order solution to Eq. (42) for the phase, we explicitly assume that the pulse shape remains unchanged. Still, our result for l_0 [Eq. (47)] is identical to the expression for the length of pulse self-steepening [22].

To gain physical insights into this finding, we consider an implicit solution to Eq. (41) [22,28]:

$$|A(\eta, z)| = \rho_0\left(\frac{\eta}{\tau_0} - Q\frac{|A(\eta, z)|^2}{I}\right), \tag{48}$$

where $\rho_0(\eta) = |A(\eta, 0)|$.

Equation (48) is instructive in showing that the peak of the pulse propagates slower (for $n_2 > 0$) or faster (for $n_2 < 0$) than the pulse edges, leading to pulse self-steepening and eventually giving rise to a shock wave in the trailing (for $n_2 > 0$) or leading (for $n_2 < 0$) edge of the pulse. As is also readily seen from Eq. (48), corrections to the pulse shape due to self-steepening are of the same order of smallness in $|Q|$ as the asymmetry of the spectral broadening. As a consequence,

the delay (advancement in materials with negative n_2) of the peak of the pulse relative to its edges, $\tau_s \approx (n_2/c)Iz$, becomes equal to the pulse width τ_0 on a typical scale, $l_s \approx c\tau_0/(n_2 I)$, equal to l_0 as defined by Eq. (47).

This is, of course, much more than a mere coincidence. That the spectral asymmetry builds up simultaneously with the pulse-shape asymmetry is a manifestation of the inseparability of the spectral-temporal mode of the field. This inseparability is lost in an iterative treatment of Eqs. (41) and (42), which searches for spectral corrections assuming no changes in the pulse shape as its first-order iteration. This hits us back in the next iteration, as we realize that the leading corrections to the pulse shape are of the same order in $|Q|$ as the corrections giving rise to spectral asymmetry. With these arguments in mind, we conclude that simultaneous conservation of energy and the photon number in nonlinear-optical processes leads to an asymmetry of spectral-temporal modes of broadband field waveforms.

VII. QUANTITATIVE ANALYSIS

As a specific example, Figs. 1–3 display the results of numerical simulations performed for ultrashort laser pulses with an initial pulse width of 180 fs, central wavelength $\lambda_0 = 3.2\,\mu\mathrm{m}$, and pulse energy $E_0 = 45\,\mu\mathrm{J}$—a typical short-pulse output of multicascade optical parametric amplifiers [32]—undergoing soliton transformations in a gas-filled antiresonance-guiding single-ring hollow-core photonic-crystal fiber (PCF) [33,34]. Fibers of this class have
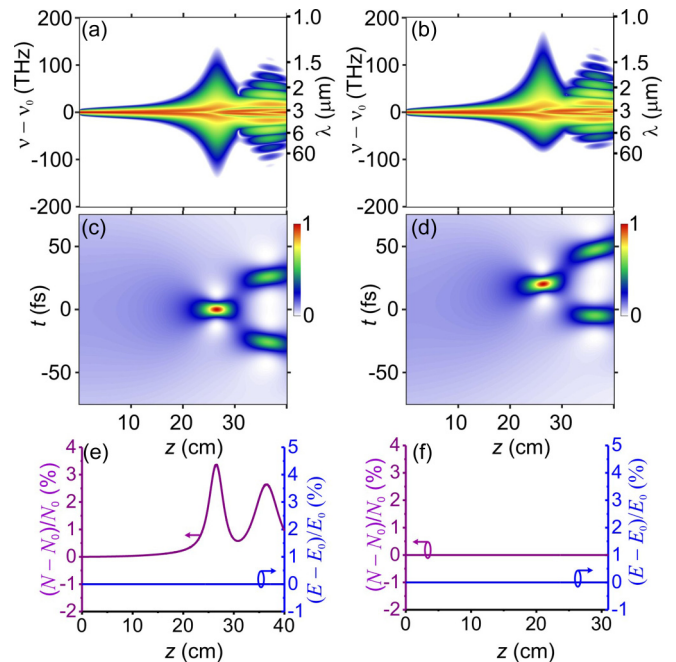

FIG. 1. Spectral (a, b) and temporal (c, d) evolution, as well as normalized photon-number $\delta N(z)/N_0$ (purple line) and energy $\delta E(z)/E_0$ (blue line) variations along z (e, f) for a laser pulse with an initial pulse width of 180 fs, central wavelength $\lambda_0 = 3.2\,\mu\mathrm{m}$, and pulse energy $E_0 = 45\,\mu\mathrm{J}$ in a hollow fiber with $\beta_2 = -55\,\mathrm{fs}^2/\mathrm{cm}$ and $\varepsilon = 1$ (corresponding to a pure Kerr nonlinearity, with no Raman effect) simulated by solving (a, c, e) the NSE [Eq. (5)] and (b, d, f) the GNSE [Eq. (3)] without high-order ($k > 2$) dispersion terms.
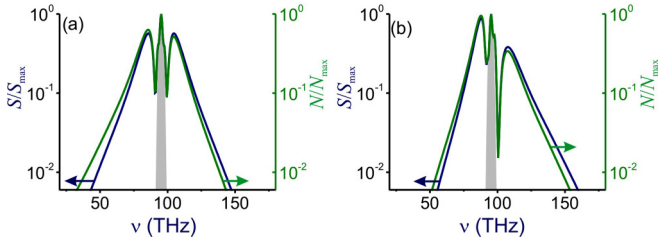
FIG. 2. The spectral intensity (blue line) and the photon number (green line) as a function of the frequency at the point of maximum pulse compression for a laser pulse with an initial pulse width of 180 fs, central wavelength $\lambda_0 = 3.2\,\mu$m, and pulse energy $E_0 = 45\,\mu$J in a hollow fiber filled with argon ($\varepsilon = 1$) at $p = 5.0$ bars. Simulations are performed by solving (a) the NSE [Eq. (5)] and (b) the GNSE [Eq. (3)] without high-order ($k > 2$) dispersion terms. The spectrum of the input field is shown by gray shading.

been shown to provide a powerful resource for multioctave supercontinuum generation in the near- and mid-infrared [35,36]. Transmission bands and dispersion of these fibers are controlled by the size of the fiber core and the geometry of the antiresonance ring structure.

Simulations presented in Figs. 1–3 were performed for an antiresonance-guiding PCF where a hollow core with a diameter $D_c \approx 70\,\mu$m is bounded by an array of six identical silica rings, each having a diameter $d \approx 37\,\mu$m and a wall with a thickness of $t \approx 0.59\,\mu$m. A fiber with such a design provides a high transmission and anomalous dispersion within the entire spectrum of 3.2-μm 180-fs pulses, allowing these pulses to be coupled into solitons inside the fiber. The fiber is filled with argon at a pressure $p = 5.0$ bars. Optical nonlinearity of argon is entirely due to the Kerr effect, i.e., $\varepsilon = 1$. The Kerr-effect nonlinear refractive index for argon is estimated as $n_2 \approx 1.35 \times 10^{-19}\,(p/p_a)\,\text{cm}^2/\text{W}$, where p_a is the atmospheric pressure. Keeping our focus on photon-number conservation, we neglect in our simulations ionization effects, which can be easily included in the GNSE [37–40]. Such effects can play a moderate role within the studied parameter space, slightly enhancing the blueshift and finely tuning phase-matching features, but do not lead to dramatic changes in field waveform dynamics [26]. Parameters of the input laser pulse, the fiber design, and the gas pressure are chosen in our simulations in such a way as to examine photon-number conservation in multioctave field waveforms. To isolate the role of the frequency dependence of nonlinear wave coupling and pulse self-steepening, the waveguide loss has been neglected in our simulations. This is a clear idealization, especially for NSE calculations, where the long-wavelength part of the spectrum is allowed to reach the far-infrared range [Fig. 1(a)] due to no low-frequency bound on spectral broadening in NSE-based models.

Numerical simulations performed with the use of the NSE, shown in Figs. 1(a) and 1(c), reveal a typical breathing soliton dynamics, as expected for pulses with a soliton number $N \approx 6$. As a part of this breathing dynamics, the stage of pulse compression and spectral broadening [$z < 26$ cm in Figs. 1(a) and 1(c)] is followed by pulse stretching and spectral compression, in which the pulse exhibits its multisoliton structure. As a typical property of NSE solutions, field waveforms with a sym-
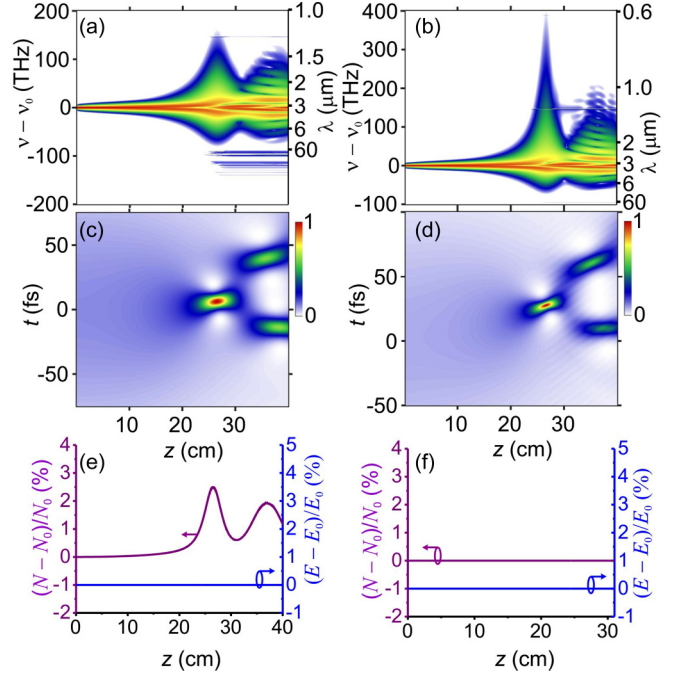

FIG. 3. Spectral (a, b) and temporal (c, d) evolution, as well as normalized photon-number $\delta N(z)/N_0$ (purple line) and energy $\delta E(z)/E_0$ (blue line) variations along z (e, f) for a laser pulse with an initial pulse width of 180 fs, central wavelength $\lambda_0 = 3.2\,\mu$m, and pulse energy $E_0 = 45\,\mu$J in a hollow fiber filled with argon ($\varepsilon = 1$) at $p = 5.0$ bars simulated by solving (a, c, e) the GNSE [Eq. (5)] with high-order ($k > 2$) dispersion terms, but with $\hat{S} = 0$ and (b, d, f) the full GNSE [Eq. (3)].

metric input pulse shape experience perfectly spectral broadening [Fig. 1(a)]. The broadest spectral bandwidth is achieved at the point of maximum pulse compression ($z \approx 26$ cm).

As the soliton pulse evolution shown in Figs. 1–3 is accompanied by pulse self-compression to pulse widths on the order of the field cycle, the applicability of pulse evolution equations (2) and (3) needs to be reexamined. These equations remain applicable even in the case of subcycle pulse widths [26,37–39] as long as ionization effects are negligible (which is the case in the considered parameter space) and the characteristic spatial scales, such as the dispersion length $l_d = \tau^2/\max\{|\beta_2(\omega)|\}$, the nonlinear length $l_{\text{NL}} = c(\omega_0 n_2 I_{\max})^{-1}$, and the self-steepening length $l_{\text{SS}} = 0.4\tau\omega_0 c(\omega_0 n_2 I)^{-1}$, meet the conditions βl_d, βl_{NL}, $\beta l_{\text{ss}} \gg 1$ within the entire frequency interval centered at ω_0 and the relative mismatch of the phase and group and velocities is small, $|\beta(\omega_0) - \omega_0\beta_1(\omega_0)|/\beta(\omega_0) \ll 1$. For the shortest pulse width in our simulations, $t \approx 3$ fs, and the maximum field intensity, $I_{\max} \approx 95\,\text{TW/cm}^2$, we find for the typical parameters of our pulse compression scenario $\beta l_d \approx 2 \times 10^3$, $\beta l_{\text{NL}} \approx 2 \times 10^4$, $\beta l_{\text{ss}} \approx 10^4$, and $|\beta(\omega_0) - \omega_0\beta_1(\omega_0)|/\beta(\omega_0) \approx 10^{-3}$. This confirms that all the applicability criteria for pulse evolution equations (2) and (3) are fulfilled.

With the NSE setting a no low-frequency bound on spectral broadening, the long-wavelength wing of the spectrum stretches at the point of maximum pulse compression all the way down to the far infrared [Figs. 1(a) and 2(a)]. Obviously, NSE predictions become unphysical in this regime. As high-

lighted in Sec. III, there is nothing in NSE-based models that would prevent the low-frequency wing of the spectrum from reaching the zero frequency—a result that is clearly at odds with the fundamental principles of electrodynamics. Although these stages of spectral broadening do not represent the actual evolution of a laser pulse, they are still shown in Figs. 1(a) and 2(a) to facilitate comparison with the predictions of the GNSE, where the unphysical low-frequency wing of the spectrum is suppressed by the optical shock wave.

Since the spectrum in NSE-based models is symmetric, the energy of the high-frequency wing of the spectrum has to be equal to the energy of the low-frequency wing [Fig. 2(a)]. With a typical energy of a photon in the far infrared being much less than the energy of a photon in the visible, this can only be achieved at a cost of extra photons [Fig. 2(a)]. To quantify this effect, we examine the behavior of the photon-number integral (21) as a function of the propagation path of the pulse. In [Fig. 1(e)], we plot the normalized photon-number variation $\delta N(z)/N_0 = [N(z) - N_0]/N_0$, where $N_0 = N(0)$, as a function of z. The deviation of $N(z)$ from N_0 is seen to exhibit a well-resolved peak centered at the point of maximum pulse compression and, hence, maximum spectral broadening. On a larger scale, $\delta N(z)$ displays oscillations, following pulse-compression—pulse stretching cycles in soliton breathing dynamics.

Importantly, while the photon number is not conserved by NSE dynamics, the energy has to remain constant as a fundamental constant of motion of the NSE. To check the invariance of energy, the normalized energy deviation $[E(z) - E_0]/E_0$, where $E(z) = \int |A(\omega_0 + \Omega, z)|^2 d\Omega$ and $E_0 = E(0)$, is also plotted in Fig. 1(e) as a function of z. As is readily seen from this plot, the energy remains constant with a very high accuracy throughout the entire NSE soliton breathing dynamics.

Figures 1(b), 1(d), 1(f), and 2(b) present simulations performed with the use of the GNSE [Eq. (3)] without high-order ($k > 2$) dispersion terms and with $\varepsilon = 1$ (the nonlinear response of argon has no Raman component anyway). This version of the GNSE is equivalent to the NSE with added $\hat{S}$ term. In this model of pulse evolution, the asymmetry of spectral broadening is lost [Figs. 1(b) and 2(b)]. Remarkably, this loss of spectral asymmetry and, hence, temporal pulse profile [Fig. 1(d)] is needed to restore the photon number $N(z)$ to its status as a constant of motion without letting the energy $E(z)$ lose this status. With the asymmetry brought into the spectral broadening by the $\hat{S}$ operator, both the photon number and the energy are conserved, as can be seen in Fig. 1(f), with a high accuracy through all the phases of the NSE soliton breathing dynamics.

Figure 3 presents the results of GNSE simulations performed with and without the $\hat{S}$ term. As a general tendency [Figs. 3(a) and 3(c)], high-order dispersion distorts the waveform and induces soliton instabilities via a resonant energy exchange between solitons and dispersive waves. Coupling between ideal NSE solitons and dispersive waves is prohibited by momentum conservation. Higher-order dispersion can, however, phase match solitons and dispersive waves, inducing intense dispersive-wave radiation. Even though these effects give rise to a spectral asymmetry and suppress the long-wavelength wing of the spectrum [cf. Figs. 1(a) and 3(a)], without the $\hat{S}$ term, they do not help conserve the number
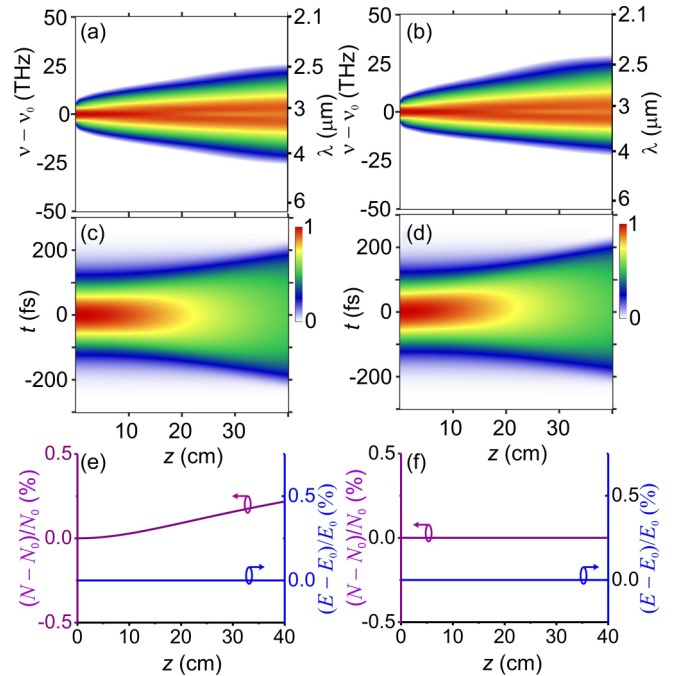

FIG. 4. The same as in Fig. 1, but with $\beta_2 = 55 \, \text{fs}^2/\text{cm}$.

of photons [Fig. 3(e)]. Although predictions of the GNSE without the $\hat{S}$ term do not represent the actual evolution of a laser pulse near the point of maximum pulse compression, we still show these stages of spectral broadening in [Fig. 3(a)] to facilitate comparison with the predictions of the full GNSE, where the unphysical low-frequency wing of the spectrum is suppressed by the optical shock wave. Even though soliton instabilities induced by high-order dispersion open a channel whereby solitons can lose both energy and photons, these effects do not change the total energy and the total photon number of the overall field, consisting of the solitonic part and nonsoliton dispersive-wave radiation, since the energy and the photon number lost by the solitonic part of the field are transferred to the dispersive wave.

Similar to NSE modeling, deviations of $N(z)$ from N_0 become dramatic near the point of maximum pulse compression, where the maximum spectral bandwidth is achieved [Figs. 3(a), 3(c), and 3(e)]. With the $\hat{S}$ term added, the short-wavelength wing of the spectrum is radically enhanced, while the low-frequency part of the spectrum is further suppressed [Fig. 3(b)], yielding a spectral-temporal mode that simultaneously conserves both the energy and the number of photons [Fig. 3(f)].

Figure 4 illustrates a typical dynamics of a laser pulse in the regime of normal dispersion. Except for the sign of β_2, which is now taken positive, $\beta_2 = 55 \, \text{fs}^2/\text{cm}$, all the parameters in these simulations are taken the same as in Fig. 1. Instead of the signature soliton breathing, observed in Fig. 1, the laser pulse in Fig. 4 undergoes temporal stretching [Figs. 4(c) and 4(d)], due to the normal dispersion, and spectral broadening [Figs. 4(c) and 4(d)], which is mainly due to SPM. At large z [$z > 30 \, \text{cm}$ in Figs. 4(b) and 4(d)], the laser pulse shape becomes asymmetric [Fig. 4(d)], while its spectrum displays a signature blueshift [Fig. 4(b)] due to the shock term in Eq. (3).

As the most important finding, we see that, similar to the case of anomalous dispersion [Figs. 3(e) and 3(f)], the NSE does not conserve the photon number [Figs. 4(e) and 4(f)]. Since the spectral bandwidth is now a monotonic function of z [Fig. 4(a)], the $\delta N(z)/N_0$ ratio calculated with the NSE also grows with z monotonically [purple line in Fig. 4(e)], while $[E(z) - E_0]/E_0$ remains constant at any z [blue line in Fig. 4(e)]. This result agrees well with Eq. (36). Similar to the regime of anomalous dispersion, with the $\hat{S}$ term added to the field evolution equation, the photon number $N(z)$ is restored in its status as a constant of motion [purple line in Fig. 4(f)] without letting the energy $E(z)$ lose this status [blue line in Fig. 4(f)].

VIII. CONCLUSION

To summarize, we have shown that the spectral and temporal symmetry of NSE solutions is inconsistent with simultaneous energy and photon-number conservation. We have demonstrated that the photon-number integral of the NSE differs from the physical number of photons, conserved by more general field evolution equations. This difficulty is traced to the optical shock term, which is dropped in the NSE, making nonlinear coupling in NSE-based models frequency independent and leading to unphysical predictions in the case of ultrabroadband, octave-spanning field waveforms.

[1] L. Mandel and E. Wolf, *Optical Coherence and Quantum Optics* (Cambridge University, Cambridge, England, 1995).

[2] M. O. Scully and M. S. Zubairy, *Quantum Optics* (Cambridge University, Cambridge, England, 1997).

[3] Y. R. Shen, *The Principles of Nonlinear Optics* (Wiley-Interscience, New York, 1984).

[4] R. Boyd, *Nonlinear Optics*, 3rd ed. (Academic, New York, 2008).

[5] A. A. Voronin, A. A. Lanin, and A. M. Zheltikov, Opt. Express **24**, 23207 (2016).

[6] V. B. Berestetskii, E. M. Lifshitz, and L. P. Pitaevskii, *Quantum Electrodynamics*, 2nd ed. (Butterworth, Washington, DC, 1982).

[7] G. S. Agarwal, *Quantum Optics* (Cambridge University, Cambridge, England, 2012).

[8] M. A. Nielsen and I. L Chuang, *Quantum Computation and Quantum Information* (Cambridge University, Cambridge, England, 2000).

[9] G. Grynberg, A. Aspect, and C. Fabre, *Introduction to Quantum Optics* (Cambridge University, Cambridge, England, 2010).

[10] A. M. Weiner, *Ultrafast Optics* (Wiley, New York, 2008).

[11] A. M. Zheltikov, A. L'Huillier, and F. Krausz, Nonlinear optics, in *Handbook of Lasers and Optics*, edited by F. Träger (Springer, New York, 2007), pp. 157–248.

[12] S. Mukamel, *Principles of Nonlinear Optical Spectroscopy* (Oxford University, New York, 1995).

[13] A. M. Zheltikov, A. A. Voronin, M. Kitzler, A. Baltuška, and M. Ivanov, Phys. Rev. Lett. **103**, 033901 (2009).

[14] J. M. Dudley, G. Genty, and S. Coen, Rev. Mod. Phys. **78**, 1135 (2006).

[15] A. M. Zheltikov, Appl. Phys. B **77**, 143 (2003)

[16] A. M. Zheltikov, Phys. Usp. **49**, 605 (2006).

[17] J. M. Dudley and J. R. Taylor, Nature Photonics **3**, 85 (2009).

[18] S. E. Harris and L. V. Hau, Phys. Rev. Lett. **82**, 4611 (1999).

[19] N. Matsuda, R. Shimizu, Y. Mitsumori, H. Kosaka, and K. Edamatsu, Nature Photonics **3**, 95 (2009).

[20] T. Peyronel, O. Firstenberg, Q. Liang, S. Hofferberth, A. V. Gorshkov, T. Pohl, M. D. Lukin, and V. Vuletić, Nature (London) **488**, 57 (2012).

[21] V. Venkataraman, K. Saha, and A. L. Gaeta, Nature Photonics **7**, 138 (2013).

[22] G. P. Agrawal, *Nonlinear Fiber Optics* (Academic, San Diego, 2001).

[23] K. J. Blow and D. Wood, IEEE J. Quantum Electron. **25**, 2665 (1989).

[24] A. M. Zheltikov, Opt. Commun. **282**, 985 (2009).

[25] A. Hasegawa, *Optical Solitons in Fibers* (Springer, Heidelberg, 1990).

[26] A. A. Voronin and A. M. Zheltikov, Phys. Rev. A **90**, 043807 (2014).

[27] L. F. Mollenauer, R. H. Stolen, and J. P. Gordon, Phys. Rev. Lett. **45**, 1095 (1980).

[28] G. Yang and Y. R. Shen, Opt. Lett. **9**, 510 (1984).

[29] H. A. Haus, *Electromagnetic Noise and Quantum Optical Measurements* (Springer, Berlin, 2000).

[30] J. M. Manley and H. E. Rowe, Proc. IRE **44**, 904 (1956).

[31] M. Weiss, Proc. IRE **45**, 1012 (1957).

[32] E. A. Stepanov, A. A. Lanin, A. A. Voronin, A. B. Fedotov, and A. M. Zheltikov, Phys. Rev. Lett. **117**, 043901 (2016).

[33] A. D. Pryamikov, A. S. Biriukov, A. F. Kosolapov, V. G. Plotnichenko, S. L. Semjonov, and E. M. Dianov, Opt. Express **19**, 1441 (2011).

[34] F. Yu and J. C. Knight, IEEE J. Sel. Topics Quantum Electron. **22**, 440610 (2016).

[35] M. Cassataro, D. Novoa, M. C. Günendi, N. N. Edavalath, M. H. Frosz, J. C. Travers, and P. St. J. Russell, Opt. Express **25**, 7637 (2017).

[36] U. Elu, M. Baudisch, H. Pires, F. Tani, M. H. Frosz, F. Köttig, A. Ermolov, P. St. J. Russell, and J. Biegert, Optica **4**, 1024 (2017).

[37] T. Brabec and F. Krausz, Phys. Rev. Lett. **78**, 3282 (1997).

[38] L. Bergé, S. Skupin, R. Nuter, J. Kasparian, and J.-P. Wolf, Rep. Prog. Phys. **70**, 1633 (2007).

[39] A. Couairon and A. Mysyrowicz, Phys. Reports **441**, 47 (2007).

[40] E. E. Serebryannikov, E. Goulielmakis, and A. M. Zheltikov, New J. Phys **10**, 093001 (2008).